Preprints (www.preprints.org) | NOT PEER-REVIEWED | Posted: 5 August 2019 doi:10.20944/preprints201908.0051.v1

Electric and Thermoelectric Properties of $Cu_{12}Sb_4S_{13}$ Tetrahedrite with Impurities

Kamyar Ravaji*

Department of Material Science and Engineering, Sharif University of Technology, Tehran, Iran. P.O. Box 11155-9466.

Reza Ezzati

Science and Research Branch, Islamic Azad University, Tehran, I. R. Iran

Amir Hosein Mohammadi

Science and Research Branch, Islamic Azad University, Tehran, I. R. Iran

Seyed Amir Abbas

Science and Research Branch, Islamic Azad University, Tehran, I. R. Iran

*Corresponding author: kamyar.ravaji@gmail.com

Abstract

The high figure of merit and earth abundance of $Cu_{12}Sb_4S_{13}$ thermoelectric materials have recently attracted many attentions toward these type of complex compounds. Intrinsic low thermal conductivity, as well as tunable electronic transport properties, make them suitable for thermoelectric power generation. In this study, we perform a comparative theoretical study on the substituted compounds, primarily at the Cu site including known tetrahedrite $Cu_{12}Sb_4S_{13}$, by means of first-principles calculations. The density functional theory of electric structure is applied to investigate the result of substitution.

Keywords: Ab initio calculation; thermoelectric materials; tetrahedrite

© 2019 by the author(s). Distributed under a Creative Commons CC BY license.

Preprints (www.preprints.org) | NOT PEER-REVIEWED | Posted: 5 August 2019 doi:10.20944/preprints201908.0051.v1

1. Introduction

The efficiency of a thermoelectric (TE) material defined by a dimensionless figure of merit, $ZT = \frac{S^2\sigma T}{\kappa} = \frac{PT}{\kappa}$, wherein σ is the electrical conductivity, P is power factor, S Seebeck coefficient and κ is the thermal conductivity. The κ includes both lattice contribution κ_L and electronic κ_e contribution κ_L , i.e. $\kappa = \kappa_e + \kappa_L$. The enhanced ZT determines the productivity of a thermoelectric material. The preeminent of the known TE materials have a value of ZT to be of the order of unity at ambient condition.[1] The ZT equation implies that finding materials with ZT more than one is an open challenge, since it is required to satisfy the conflicting tie of high $P = S^2\sigma$ resembling an insulator and simultaneously behave as a decent conductor like a metal. High ZT indicates that a good TE material should have high electrical conductivity σ and low thermal conductivity κ leading to large phonon scattering and small electron scattering. In last couple of years, a lot of efforts have been made to study thermoelectric materials and develop new methods to enhance the value of the ZT. Multiple reports have been published by various groups with a focus on studying atomic structure and electronic behavior leading to low thermal conductivity[2, 3]. In addition, several studies performed on band structure engineering to improve Seebeck coefficient and electric conductivity and implementing nanostructure technology for decreasing the lattice thermal conductivity[4, 5]. There has been some research on the effect of Kondo correlations on the thermopower[6, 7, 8, 9, 10, 11, 12].

Recently, several studies focused on multiple-filled skutterudites[13, 14]. Xun Shi et al,[14] reported that there are a few doped samples which show an improved figure of merit of 1.7 at around 850 K. This ZT is one of the highest value reported in skutterudites type of TE materials. Furthermore, Biswas et al.,[15] found high-performance bulk thermoelectrics ZT 2.2 value at 923 K for p-type PbTe-SrTe doped with Na. This high value of ZT is assigned to the hierarchical structure which enhances the phonon scattering.

Several restrictions such as toxicity and scarcity of the elements limit de-

Preprints (www.preprints.org) | NOT PEER-REVIEWED | Posted: 5 August 2019 doi:10.20944/preprints201908.0051.v1

velopment of capable thermoelectric materials in large scale in industrial utilization. However, the search for promoting thermoelectric compounds goes on in spite of these constraints. Lately, new natural minerals of tetrahedrite paved the road for new successes in developing new thermoelectric materials. Tetrahedrite ($Cu_{12-x}\alpha_xSb_4S_{13}$) and tennantite ($Cu_{12-x}\alpha_xAs_4S_{13}$), where α is a transition metal element such as Zn, Co, Fe, Mn, and Ni, have attracted much attention because their thermal conductivity is very low due to phonon scattering by the so-called rattling motion, which is the large-amplitude atomic motion.[16, 17, 18, 19, 20, 2]. These studies have motivated us to explore electronic and thermoelectric features of tetrahedrite family of thermoelectric materials.

Considering a trivial ionic picture, all the copper atoms in tetrahedrites are assumed to be monovalent and contribute just only one electron. Other divalent substitutes like Mn provide two electrons, as S and Sb atoms provide six and three electrons, respectively. Accordingly, from $Cu_{12}Sb_4S_{13}$ to $Cu_{10}Zn_2Sb_4S_{13}$, the valence electron count enhances four electrons per unit cell.

In this work, we study and compare the electronic structure of substituted tetrahedrite with other group of tetrahedrites substituted by some other elements. The electronic structure was obtained by implementing a DFT calculation of Wien2k program[21] and the BoltzTrap package based on the Boltzmann transport theory.[22] It has already been reported that the bands crossing the Fermi level are primarily consist up of d-orbitals of copper atoms.[23, 24, 25] Hence, in order to determine the substitution impact of a equal amount of doping for electronic structure calculations, equal amount of d-orbital occupancy is considered for parent compound of $Cu_{12}Sb_4S_{13}$.

2. Methodology

First principle density functional theory (DFT) calculations were carried out in the WIEN2k.[21] by a technique that uses Full Potential Linear Augmented plane wave (FPLAPW) as well as Plane wave self consistent field (Pwscf). The

Preprints (www.preprints.org) | NOT PEER-REVIEWED | Posted: 5 August 2019 doi:10.20944/preprints201908.0051.v1

FPLAPW is implemented to investigate the transport and electronic properties of the tetrahedrites while the bond lengths and structure optimizations were done by using Pwscf method. The Generalized Gradient Approximation (GGA) of Perdew Burke Ernzerhof (PBE)[26] was used to attain the total energy by self consistently solving the Kohn-Sham equations.

A variable cell optimization carried out by implementing conjugate gradient method as employed in Pwscf. A $9 \times 9 \times 9$ k points mesh used in the reciprocal space of the first Brillouin zone based on Monkhorst-Pack scheme[27] to guarantee a decent convergence. A plane wave cut off energy of 100 eV is applied.

The FP-LAPW method is employed as described in the WIEN2k code[21]. The standard local scheme of the exchange-correlation functional (LDA or GGA) used in the first principles calculations commonly underestimate the band gap and they can't predict precisely the localized electrons in d orbitals and sometimes in f orbitals, in DFT calculations involving transition metals[28]. To resolve this problem, we have implemented the onsite Coulomb repulsion U combined with Generalized Gradient Approximation (GGA) (GGA+U). Furthermore, several physical properties such as thermopower (S) and electrical conductivity σ and electron relaxation time τ have calculated utilizing BOLTZTRAP[22] package with various k points up to 5000 k-points. In our calculation we used the Constant Scattering Time (τ) Approximation (CSTA) along with the Rigid Band Approximation (RBA)[29] . The equations used in the calculations for electric part of thermal conductivity (κ), electrical conductivity (σ), and Seebeck coefficient (S), obey the following relations:

$$\sigma_{i,j} = \frac{e^2\tau}{\hbar^2} \int \frac{\partial\varepsilon}{\partial k_i}\frac{\partial\varepsilon}{\partial k_j}[-\frac{\partial f_\mu(T;\varepsilon)}{\partial\varepsilon}]\partial\varepsilon \tag{1}$$

$$\kappa_{i,j} = \frac{\tau}{\hbar^2 T} \int \frac{\partial\varepsilon}{\partial k_i}\frac{\partial\varepsilon}{\partial k_j}(\varepsilon-\mu)^2[-\frac{\partial f_\mu(T;\varepsilon)}{\partial\varepsilon}]\partial\varepsilon \tag{2}$$

$$S_{i,j} = \frac{1}{eT}\frac{\int \frac{\partial\varepsilon}{\partial k_\beta}\frac{\partial\varepsilon}{\partial k_j}(\varepsilon-\mu)[\frac{\partial f_\mu(T;\varepsilon)}{\partial\varepsilon}]\partial\varepsilon}{\int \frac{\partial\varepsilon}{\partial k_\beta}\frac{\partial\varepsilon}{\partial k_i}[\frac{\partial f_\mu(T;\varepsilon)}{\partial\varepsilon}]\partial\varepsilon} \tag{3}$$

where ε is is energy, T is the temperature, μ is the chemical potential, τ is a relaxation time and e is the electron charge .

Preprints (www.preprints.org) | NOT PEER-REVIEWED | Posted: 5 August 2019 doi:10.20944/preprints201908.0051.v1

Based on the RBA approximation, although adding some impurities to a system will not modify its band structure, the chemical potential will be adjusted. This could be utilized to approximate semiconductors that are not heavily doped in order to calculate some of the the transport properties theoretically.[30, 31, 32, 33] Nevertheless, adding some specific types of dopant will severely alter the nature of electronic structure below and above the gap leading to resonant states[34, 35] in which case the RBA approximation fail to predict precisely.[36] According to constant scattering time approximation (CSTA), the scattering time for an electron regardless of its energy relies only on temperature and concentration of electrons.[37] The CSTA approximation has effectively predicated the thermoelectric quantities in several different materials which were in good agreement with experimental reports.[38, 39]

3. Result and discussion

3.1. Ground state properties

The $Cu_{12}Sb_4S_{13}$ crystallize in a cubical form with space group of 217 ($I\bar{4}3m$) wherein half of the Cu atoms occupy four-coordinate distorted tetrahedral sites (Cu1) and other half occupy three-coordinate triangular sites (Cu2) with total 58 atoms per unit cell. Therefore, half of 24 Cu sites are occupied by twelve Cu-I sites and other half by twelve Cu-II sites. Figure 1 shows the calculated density of states. Spin polarization was included in the calculations. The $Cu_{12}Sb_4S_{13}$ structure lead to nonmagnetic compound. However, as expected for transition metals, the calculations converged to spin polarized kind of density of states at valence band. The role of Cu-II near the Fermi level is smaller than states formed by bonding between Cu-I and S atoms. Zinc and manganese doping will not affect the density of states, since they are far from the Fermi level. However, they will replace the Cu-I and loosen the Cu-II and sulfur's bonding and influence the density of states near the Fermi level. We have implemented the space group symmetry 81, in order to enhance the symmetry and reduce calculation time. In this symmetry space group, multiplicity of each copper site

Preprints (www.preprints.org) | NOT PEER-REVIEWED | Posted: 5 August 2019 doi:10.20944/preprints201908.0051.v1

is broken into four and two where each Zn and Mn elements can be replaced in two multiplicity positions. The calculation was carry out with considering spin polarization. Force minimization was also considered during the calculations.

The derived density of state (DOS) is illustrated in figure 1. It can be seen that the Cu states strongly hybridized with the S states which sits at the top of the valence-band. While we we note that the chalcogen p-orbitals are always strongly hybridized with them. Because of the existence of the insulating layers, the conduction along the z-direction is almost prohibited, at least near the valence-band top as inferred from the flat band dispersion along the Γ line shown in figure 1). Bands exists near the top of the valence-band at Γ point. Therefore, the valence-band structure near its edge can be regarded as quasi-one-dimensional. Such a low dimensionality is a key aspect for obtaining a good thermoelectric performance because it increases the DOS near the band edge and therefore the PF.

The flat characteristic band feature near the Fermi level indicates favorable thermopower (Seebeck coefficient) for TE applications. Since LDA/GGA underestimate the band gaps in semiconductors and insulators, and as the studied Mn have partially filled d levels, we used GGA+U method and adjusted U to get a reasonable value of the band gap. In our calculations we have used a value of $U_{Mn} = 0.6Ry$ for the Mn d-electrons.

In order to better estimate electron relaxation time $\tau_{electron}$ and lattice thermal conductivity, it is required to separated into following two terms

$$ZT = T\frac{\sigma S^2}{\kappa_e}\frac{1}{1+\frac{\kappa_L}{\kappa_e}} \tag{4}$$

where, the first term $T\frac{\sigma S^2}{\kappa_e}$ can be replaced by a factor α and the second term $\frac{1}{1+\frac{\kappa_L}{\kappa_e}}$ can be replaced by another factor β. DFT calculation for electrons will produce α, while since β includes τ_e and κ_L, it cannot derived from DFT calculations for electrons. To resolve this problem, the equation

$$\frac{\kappa_L}{\tau_L} = \frac{1}{3}C_L v_L^2 \frac{\tau_L}{\tau_e} \tag{5}$$

is being used. Where, v_L is the phonon group velocity, C_L the specific heat of

Preprints (www.preprints.org) | NOT PEER-REVIEWED | Posted: 5 August 2019 doi:10.20944/preprints201908.0051.v1

the lattice, and τ_L the phonon relaxation time.

The correlation between κ_e and σ is expressed by Wiedeman-Franz law which is being used to reduce ZT form

$$(ZT)_{Max} = (ZT)_e = T\frac{\sigma S^2/\tau_e}{LT\sigma/\tau_e} = \frac{S^2}{L} \tag{6}$$

Where, κ_e is being replaced from $\kappa_e = LT\sigma = 2.44 \times 10^{-2} mV^2/K^2$. Considering this assumption, DFT calculation for Seebeck S coefficient and thermal and electrical conductivities will result in ZT for doped tetrahedrite materials. Figure 2 shows the calculated ZT, S and $\frac{\kappa_e}{L\sigma T}$ for studied materials. The ZT is highest for $Cu_{10}Zn_2Sb_4S_{13}$ as S.

The comparison with experimental data[20] shows that calculated ZT and S are slightly smaller than the observed values. However, the increasing tendency for S is in good agreement. Similar to S increasing trend in Lorentz number observed which partially pulls off the effect on ZT.

4. Conclusions

The structural and electronic transport properties of three doped tetrahedrite are studied using density functional theory. The Seebeck S coefficient calculated using the BoltzTrap program is positive for all three tetrahedrite compounds studied here. Electronic structure calculations show that all the investigated compounds are indirect band gap semiconductors, in good agreement with earlier reports. We further calculated the thermoelectric properties of the these compounds and compared with the available experimental reports. The calculations show all the investigated compounds to be very good thermoelectric materials for p-type doping.

5. Acknowledgment

We would like to thank the Sharif University of Technology for financial support under Grant No. G960204.

Preprints (www.preprints.org) | NOT PEER-REVIEWED | Posted: 5 August 2019 doi:10.20944/preprints201908.0051.v1

References

[1] D. M. Rowe, CRC handbook of thermoelectrics, CRC press, 1995.

[2] N. Ghassemi, X. Lu, J. Ross, Nmr study of local structures and anharmonic phonon behavior in tetrahedrite thermoelectrics., in: APS Meeting Abstracts, 2018.

[3] K. Suekuni, K. Tsuruta, M. Kunii, H. Nishiate, E. Nishibori, S. Maki, M. Ohta, A. Yamamoto, M. Koyano, High-performance thermoelectric mineral cu12- x ni x sb4s13 tetrahedrite, Journal of Applied Physics 113 (4) (2013) 043712.

[4] F.-H. Sun, J. Dong, H. Tang, P.-P. Shang, H.-L. Zhuang, H. Hu, C.-F. Wu, Y. Pan, J.-F. Li, Enhanced performance of thermoelectric nanocomposites based on cu12sb4s13 tetrahedrite, Nano Energy 57 (2019) 835–841.

[5] Y. Zheng, Q. Zhang, X. Su, H. Xie, S. Shu, T. Chen, G. Tan, Y. Yan, X. Tang, C. Uher, et al., Mechanically robust bisbte alloys with superior thermoelectric performance: a case study of stable hierarchical nanostructured thermoelectric materials, Advanced Energy Materials 5 (5) (2015) 1401391.

[6] Z. Li, C. Xiao, H. Zhu, Y. Xie, Defect chemistry for thermoelectric materials, Journal of the American Chemical Society 138 (45) (2016) 14810–14819.

[7] T. A. Costi, V. Zlatić, Thermoelectric transport through strongly correlated quantum dots, Phys. Rev. B 81 (2010) 235127. doi:10.1103/PhysRevB.81.235127.
URL https://link.aps.org/doi/10.1103/PhysRevB.81.235127

[8] S. Hemmatiyan, M. R. Movassagh, N. Ghassemi, M. Kargarian, A. Rezakhani, A. Langari, Quantum phase transitions in the kondo-necklace model: perturbative continuous unitary transformation approach, Journal of Physics: Condensed Matter 27 (15) (2015) 155601.

Preprints (www.preprints.org) | NOT PEER-REVIEWED | Posted: 5 August 2019 doi:10.20944/preprints201908.0051.v1

[9] B. Sothmann, R. Sánchez, A. N. Jordan, Thermoelectric energy harvesting with quantum dots, Nanotechnology 26 (3) (2014) 032001.

[10] N. Ghassemi, S. Hemmatiyan, M. Rahimi Movassagh, M. Kargarian, A. T. Rezakhani, A. Langari, Quantum phase transitions in the kondo-necklace model, in: APS Meeting Abstracts, 2015.

[11] H. Nghiem, T. Costi, Time evolution of the kondo resonance in response to a quench, Physical review letters 119 (15) (2017) 156601.

[12] A. Bhattacharjee, B. Coqblin, Thermoelectric power of compounds with cerium: Influence of the crystalline field on the kondo effect, Physical Review B 13 (8) (1976) 3441.

[13] Y. Tian, A. A. Sirusi, S. Ballikaya, N. Ghassemi, C. Uher, J. H. Ross, Charge-carrier behavior in ba-, sr- and yb-filled $cosb_3$: Nmr and transport studies, Phys. Rev. B 99 (2019) 125109. doi:10.1103/PhysRevB.99.125109.
URL https://link.aps.org/doi/10.1103/PhysRevB.99.125109

[14] X. Shi, J. Yang, J. R. Salvador, M. Chi, J. Y. Cho, H. Wang, S. Bai, J. Yang, W. Zhang, L. Chen, Multiple-filled skutterudites: high thermoelectric figure of merit through separately optimizing electrical and thermal transports, Journal of the American Chemical Society 133 (20) (2011) 7837–7846.

[15] K. Biswas, J. He, I. D. Blum, C.-I. Wu, T. P. Hogan, D. N. Seidman, V. P. Dravid, M. G. Kanatzidis, High-performance bulk thermoelectrics with all-scale hierarchical architectures, Nature 489 (7416) (2012) 414.

[16] G. Slack, Solid state physics vol 34 ed h ehrenreich, F Seitz and D Turnbull (New York: Academic) pp (1979) 1–71.

[17] N. Ghassemi, X. Lu, X. Zhou, Y. Yan, Y. Tian, J. Ross, Nmr study of doped tetrahedrite thermoelectric materials., Bulletin of the American Physical Society.

Preprints (www.preprints.org) | NOT PEER-REVIEWED | Posted: 5 August 2019 doi:10.20944/preprints201908.0051.v1

[18] X. Lu, D. T. Morelli, Natural mineral tetrahedrite as a direct source of thermoelectric materials, Physical Chemistry Chemical Physics 15 (16) (2013) 5762–5766.

[19] N. Ghassemi, X. Lu, Y. Tian, E. Conant, Y. Yan, X. Zhou, J. H. Ross Jr, Structure change and rattling dynamics in cu12sb4s13 tetrahedrite: an nmr study, ACS applied materials & interfaces 10 (42) (2018) 36010–36017.

[20] X. Lu, D. T. Morelli, Y. Xia, F. Zhou, V. Ozolins, H. Chi, X. Zhou, C. Uher, High performance thermoelectricity in earth-abundant compounds based on natural mineral tetrahedrites, Advanced Energy Materials 3 (3) (2013) 342–348.

[21] P. Blaha, K. Schwarz, G. K. Madsen, D. Kvasnicka, J. Luitz, wien2k, An augmented plane wave+ local orbitals program for calculating crystal properties.

[22] G. K. Madsen, D. J. Singh, Boltztrap. a code for calculating band-structure dependent quantities, Computer Physics Communications 175 (1) (2006) 67–71.

[23] K. Suekuni, Y. Tomizawa, T. Ozaki, M. Koyano, Systematic study of electronic and magnetic properties for cu12–x tm x sb4s13 (tm= mn, fe, co, ni, and zn) tetrahedrite, Journal of Applied Physics 115 (14) (2014) 143702.

[24] Y. Bouyrie, C. Candolfi, V. Ohorodniichuk, B. Malaman, A. Dauscher, J. Tobola, B. Lenoir, Crystal structure, electronic band structure and high-temperature thermoelectric properties of te-substituted tetrahedrites cu 12 sb 4- x te x s 13 (0.5 x 2.0), Journal of Materials Chemistry C 3 (40) (2015) 10476–10487.

[25] X. Lu, W. Yao, G. Wang, X. Zhou, D. Morelli, Y. Zhang, H. Chi, S. Hui, C. Uher, Band structure engineering in highly degenerate tetrahedrites through isovalent doping, Journal of Materials Chemistry A 4 (43) (2016) 17096–17103.

Preprints (www.preprints.org) | NOT PEER-REVIEWED | Posted: 5 August 2019 doi:10.20944/preprints201908.0051.v1

[26] J. Perdew, K. Burke, M. Ernzerhof, Perdew, burke, and ernzerhof reply, Physical Review Letters 80 (4) (1998) 891.

[27] H. J. Monkhorst, J. D. Pack, Special points for brillouin-zone integrations, Physical review B 13 (12) (1976) 5188.

[28] R. M. Nieminen, Topics in applied physics: Theory of defects in semiconductors (2006).

[29] T. Scheidemantel, C. Ambrosch-Draxl, T. Thonhauser, J. Badding, J. Sofo, Transport coefficients from first-principles calculations, Physical Review B 68 (12) (2003) 125210.

[30] L. Jodin, J. Tobola, P. Pecheur, H. Scherrer, S. Kaprzyk, Effect of substitutions and defects in half-heusler FeVSb studied by electron transport measurements and kkr-cpa electronic structure calculations, Phys. Rev. B 70 (2004) 184207. doi:10.1103/PhysRevB.70.184207.
URL https://link.aps.org/doi/10.1103/PhysRevB.70.184207

[31] L. Chaput, P. Pécheur, J. Tobola, H. Scherrer, Transport in doped skutterudites: Ab initio electronic structure calculations, Phys. Rev. B 72 (2005) 085126. doi:10.1103/PhysRevB.72.085126.
URL https://link.aps.org/doi/10.1103/PhysRevB.72.085126

[32] D. Bilc, S. Mahanti, M. G. Kanatzidis, Electronic transport properties of pbte and agpb m sbte 2+ m systems, Physical Review B 74 (12) (2006) 125202.

[33] J. M. Ziman, Electrons and phonons: the theory of transport phenomena in solids, Oxford university press, 2001.

[34] D. Bilc, S. Mahanti, E. Quarez, K.-F. Hsu, R. Pcionek, M. G. Kanatzidis, Resonant states in the electronic structure of the high performance thermoelectrics a g p b m s b t e 2+ m: The role of ag-sb microstructures, Physical review letters 93 (14) (2004) 146403.

Preprints (www.preprints.org) | NOT PEER-REVIEWED | Posted: 5 August 2019 doi:10.20944/preprints201908.0051.v1

[35] S. Ahmad, K. Hoang, S. Mahanti, Ab initio study of deep defect states in narrow band-gap semiconductors: Group iii impurities in pbte, Physical review letters 96 (5) (2006) 056403.

[36] M.-S. Lee, S. D. Mahanti, Validity of the rigid band approximation in the study of the thermopower of narrow band gap semiconductors, Physical Review B 85 (16) (2012) 165149.

[37] K. P. Ong, D. J. Singh, P. Wu, Analysis of the thermoelectric properties of n-type zno, physical review B 83 (11) (2011) 115110.

[38] G. K. Madsen, K. Schwarz, P. Blaha, D. J. Singh, Electronic structure and transport in type-i and type-viii clathrates containing strontium, barium, and europium, Physical Review B 68 (12) (2003) 125212.

[39] T. Bither, C. Prewitt, J. Gillson, P. Bierstedt, R. Flippen, H. Young, New transition metal dichalcogenides formed at high pressure, Solid State Communications 4 (10) (1966) 533–535.

Preprints (www.preprints.org) | NOT PEER-REVIEWED | Posted: 5 August 2019 doi:10.20944/preprints201908.0051.v1

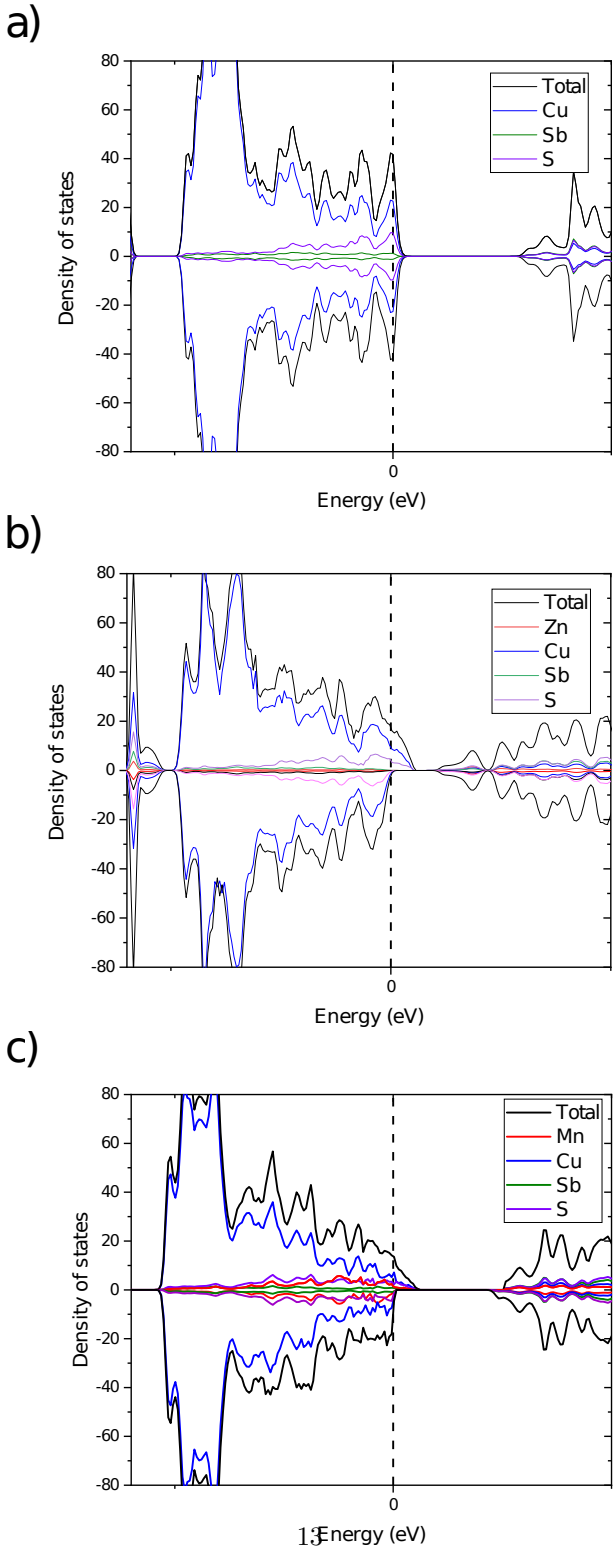

Figure 1: Calculated total and partial density of states (DOS) of (a) $Cu_{12}Sb_4S_{13}$, (b) $Cu_{10}Zn_2Sb_4S_{13}$, (c) $Cu_{10}Mn_2Sb_4S_{13}$

Preprints (www.preprints.org) | NOT PEER-REVIEWED | Posted: 5 August 2019 doi:10.20944/preprints201908.0051.v1

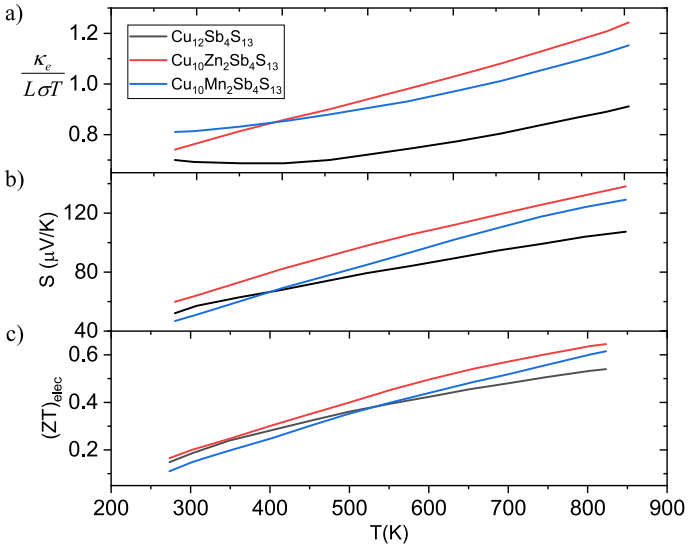

Figure 2: (a) The thermal conductivity divided by the electrical conductivity σ normalized to Lorenz number and temperature (b) Seebeck coefficient, and (c) $(ZT)_{elec}$ calculated by the BoltzTrap program using band structure obtained by a GGA+U calculation for $Cu_{12}Sb_4S_{13}$, $Cu_{10}Zn_2Sb_4S_{13}$, and $Cu_{10}Mn_2Sb_4S_{13}$.